Catalysis Today 139 (2009) 280–290

Contents lists available at ScienceDirect

Catalysis Today

journal homepage: www.elsevier.com/locate/cattod

Recent progress in selective CO removal in a H_2-rich stream

Eun Duck Park [a,*], Doohwan Lee [b], Hyun Chul Lee [b]

[a] Division of Energy Systems Research and Division of Chemical Engineering and Materials Engineering, Ajou University, Wonchun-Dong, Yeongtong-Gu, Suwon 443-749, Republic of Korea
[b] Energy and Environment Laboratory, Samsung Advanced Institute of Technology (SAIT), P.O. Box 111, Suwon 440-600, Republic of Korea

ARTICLE INFO

Article history:
Available online 6 August 2008

Keywords:
Membrane
Pd
H_2 separation
CO methanation
CO oxidation
PROX
PEMFC

ABSTRACT

In this review, recent works related to the selective CO removal in a H_2-rich stream for the application of the low-temperature fuel cell are discussed. The membrane separation, the selective CO hydrogenation, and the preferential CO oxidation (PROX) have been generally studied to meet the requirement for the polymer electrolyte membrane fuel cell (PEMFC) where the CO concentration should be controlled to be less than 10 ppm not to degrade the electrochemical performance of Pt anode. For the membrane separation, the thin layer of Pd-based alloy metal on the porous ceramic material coupled with the catalytic purification is the most advanced method at present. For PROX catalysts, supported Ru catalysts and Pt-based alloy catalysts have been successfully developed so far. The combination of highly selective PROX catalysts and the CO methanation catalyst can provide the extended temperature range to achieve the acceptable CO removal. Because each method has presently its own weak points, the further advance is still in need. The non-noble metal-based membrane requiring smaller pressure differentials is highly plausible in the membrane separation. The highly selective catalyst for CO methanation in the presence of excess CO_2 and H_2O can simplify the CO removal step. The PROX catalyst should be operative over a wide reaction temperature as well as at low temperatures not to cause the reverse water–gas shift reaction. During the development of these catalysts, the progress on the high-temperature PEM fuel cell or the CO-tolerant anode should be carefully evaluated.

1. Introduction

Fuel cells which convert chemical energy directly into electrochemical energy with high efficiency and low emission of pollutants encompass the alkaline fuel cell (AFC), the polymer-electrolyte-membrane fuel cell (PEMFC), the phosphoric-acid fuel cell (PAFC), the molten-carbonate fuel cell (MCFC), and the solid-oxide fuel cell (SOFC) [1]. Each fuel cell has its own characteristics such as the operating temperature, kinds of fuel and electrolyte. Among them, the PEMFC, which is typically operating around 80 °C with H^+ as a charge carrier, has been attracting much attention in the application to electric vehicles or residential power-generations because of its many attractive features such as high power density, rapid start-up, and high efficiency. Because this PEMFC utilizes hydrogen as a fuel, the fuel processor is in need to convert various hydrocarbons into hydrogen via a couple of catalytic reactions such as a steam reforming and a water–gas shift reaction [2–8]. The water–gas shift reaction ($CO + H_2O \leftrightarrow CO_2 + H_2$) is exothermic and thermodynamically limited. Therefore, the high CO conversion only can be obtained at low temperatures. Fig. 1 shows the exit equilibrium CO concentration depending on the inlet feed composition such as H_2O/CO ratio and the reaction temperature [9]. The CO concentration below 100 ppm cannot be achieved only via the water gas shift reaction even with the high H_2O/CO ratio at reaction temperature above 470 K. Furthermore, conventional water–gas shift catalysts show low catalytic activities at low temperatures [8,10]. Therefore, about 1 vol% of carbon monoxide is usually contained in the hydrogen stream after the water–gas shift reactor. Since platinum, an anode of PEMFC, is prone to be poisoned in the presence of small amounts of CO in the hydrogen stream, carbon monoxide should be removed to a trace-level [11]. The acceptable CO concentration is below 10 ppm at Pt anode and below 100 ppm at CO-tolerant alloy anodes [12]. Two different approaches have been investigated to remove CO in a H_2-rich stream, such as hydrogen separation including cryogenic separation, pressure swing adsorption and selective diffusion and catalytic transformation of CO into CH_4 or CO_2. For the application of small-scale fuel processor, the selective diffusion, the selective CO methantion, and the preferential CO oxidation (PROX) have been considered to be promising. Recent progress on these topics is covered in this work.

---

* Corresponding author. Tel.: +82 31 219 2384; fax: +82 31 219 1612.
E-mail address: edpark@ajou.ac.kr (E.D. Park).

0920-5861/$ – see front matter © 2008 Elsevier B.V. All rights reserved.
doi:10.1016/j.cattod.2008.06.027

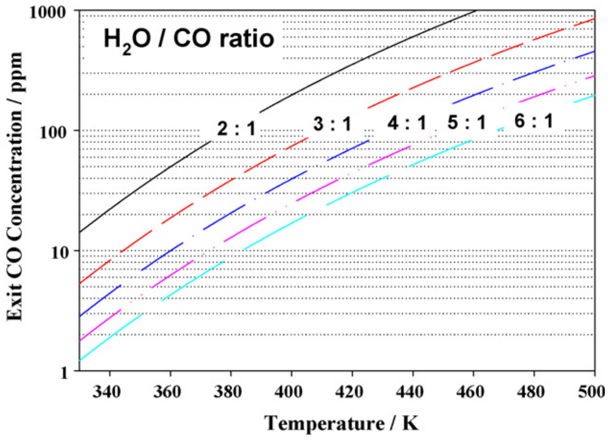

Fig. 1. The calculated equilibrium CO concentration at different temperatures with different initial H_2O/CO ratios.

2. Selective diffusion of H_2 through the membrane

Various types of membranes from polymeric constituents to inorganic ones such as dense phase metal including metal alloys and porous ceramic materials have been applied to purify H_2 [13,14]. To meet the requirements of PEMFC feed such as a high permselectivity for H_2 and a high H_2 permeability, the dense phase metal membrane in which the solution diffusion is dominant has been considered to be most plausible. Among them, the Pd metal has been well known as the representative material for hydrogen separation because of its high hydrogen permeability, good mechanical characteristics and highly catalytic surface. The permeation of hydrogen through Pd involves following three steps [14].

(1) Reversible dissociative chemisorption of hydrogen on the Pd surface.
(2) Reversible dissolution of surface atomic hydrogen in the bulk layers of the Pd.
(3) Diffusion of atomic hydrogen in the membrane.

This causes the extremely high selectivity for hydrogen separation compared with those of other size-selective membrane separation methods. Because the pure Pd membrane becomes brittle after a few cycles of $\alpha \leftrightarrow \beta$ transitions at the temperature below 300 °C and pressure $<$20 MPa [15–17], Pd-based alloys such as Pd–Ag and Pd–Cu have been generally adopted as the membrane material. The bulk diffusion is often the rate-limiting step, which can be facilitated by increasing pressure differentials as well as the operating temperature. The hydrogen flux can also be increased by decreasing the membrane thickness, which has the positive effect on the cost control as well. Further decrease in the expensive Pd metal has been achieved by deposition of thin layer of Pd-based alloy metal on the porous ceramic material [18]. However, this suffers from the fatal flaw of "pinhole" short circuit paths, which will allow for other species to pass directly through the membrane thus reducing the purification factor of the membrane [19]. Recently, a composite comprising a hydrogen diffusion membrane and a methanation catalyst has been claimed to be effective to cope with this problem [20].

There are several advantages of membrane separation as follows [21].

(1) The fuel cell becomes smaller and cheaper because pure hydrogen can be fed to it.
(2) Fuel cell can run without the bleed-out of the anode gas from the stack, which maximizes the hydrogen utilization.
(3) The system can be simplified because various components required in the PROX system to control the heat and the air-injection rate is not necessary.

There is another room to reduce space and weight of the fuel processor if a reformer and membrane module is combined as shown in Fig. 2. The hydrogen, which does not permeate, and the carbon monoxide are converted in a catalytic burner into heat and utilized for the endothermic reforming process.

The development of non-palladium-based membranes that offer a lower cost, high flux, and high durability is still demanding. V-, Nb- and Ta-based alloy metals have been proposed and intensively investigated as the possible candidates [22,23].

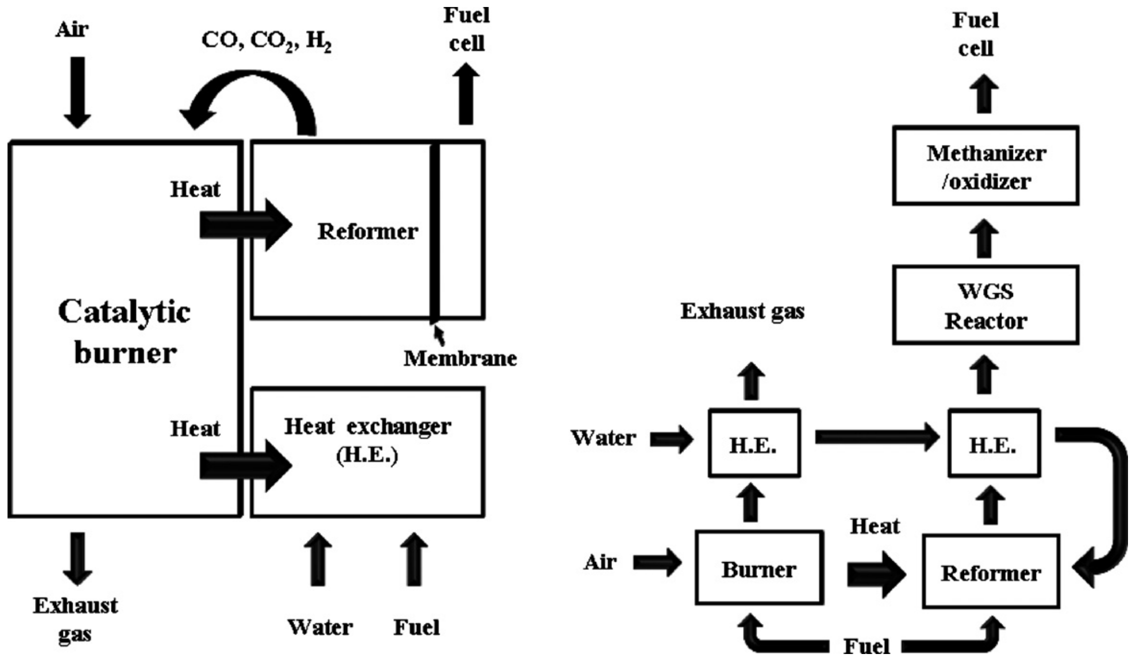

Fig. 2. The schematic diagram of the fuel processor incorporated with the membrane reactor concept (left-hand side) or the catalytic purification (right-hand side).

3. Selective CO methanation

The following reactions can be carried out over the hydrogenation catalyst in the presence of CO, CO_2, and H_2 which are main gaseous components in the exit of water–gas shift reactor.

$$CO(g) + 3H_2(g) \rightarrow CH_4(g) + H_2O(g) \quad \Delta H^{\circ}_{298} = -205,813\ \mathrm{J/mol} \tag{1}$$

$$CO_2(g) + 4H_2(g) \rightarrow CH_4(g) + 2H_2O(g) \quad \Delta H^{\circ}_{298} = -164,647\ \mathrm{J/mol} \tag{2}$$

The selective CO methanation (Eq. (1)) can be promising because this does not require the introduction of any gases such as air in the PROX system. Ru or Rh supported on an alumina [24] and Ru/TiO_2 [25] were claimed to be effective for the selective CO methanation in the presence of CO_2. Rehmat and Randhava [26] compared some commercial catalysts such as $Ru/\alpha\text{-}Al_2O_3$, Raney nickel and alumina-supported Ni catalysts and found that Ru was the most effective, followed closely by the Raney nickel-type catalyst. Takenaka et al. proposed Ni/ZrO_2 and Ru/TiO_2 as promising catalysts based on the screening experiment and concluded that the larger Ni and the smaller Ru was plausible for the high catalytic activity [27]. They also showed that the CO concentration can be decreased from 0.5% to 20 ppm in the gases formed by the steam reforming of methane. Echigo and Tabata [28] reported that the CO concentration below 10 ppm could be obtained only by multi-stage CO methanation over Ru/Al_2O_3. Some catalysts for this reaction and their performance are summarized in Table 1. Even though most previous works were conducted with rather low inlet CO concentration below 0.5 vol%, the acceptable CO concentration below 10 ppm cannot be obtained. The H_2 consumption as well as the exit CO concentration in ppm levels should be reported to be comparable with the competing PROX system in future works.

There are some obstacles to be overcome in this system as follows.

(1) The temperature window showing high CO conversion is very narrow even in the lab-scale experiments. This can cause severe problems in the scale-up process because this reaction is highly exothermic.
(2) The reaction temperature is still relatively high for the reverse water–gas shift reaction to occur, which can cause the unacceptable CO concentration at low space velocities frequently encountered in the cyclic operation.
(3) The rapid consumption of hydrogen can be carried out via the CO_2 methanation in the absence of the fine temperature control.
(4) The inlet CO concentration should be low to reduce CO concentration satisfactorily, which requires a large amount of water–gas shift catalyst.

4. Preferential CO oxidation

The carbon monoxide in the exit of the water–gas shift reactor can be removed over the oxidation catalyst with the oxygen supplied externally. Although this PROX system requires the units to control the temperature and the flow rate of air, the smaller amounts of hydrogen can be consumed compared with those of the selective CO methantion. The following reactions can be carried out in the PROX system.

$$CO(g) + \tfrac{1}{2}O_2(g) \rightarrow CO_2(g) \quad \Delta H^{\circ}_{298} = -282,984\ \mathrm{J/mol} \tag{3}$$

$$H_2(g) + \tfrac{1}{2}O_2(g) \rightarrow H_2O(g) \quad \Delta H^{\circ}_{298} = -241,818\ \mathrm{J/mol} \tag{4}$$

In the earlier works, the PROX catalyst was sought to be applied to purify the hydrogen for the application of ammonia synthesis. Supported Pt, Ru, and Rh were appeared to be effective and the supported Pt catalyst was evaluated on reformer gas in a pilot plant [31]. The supported Pt catalyst was claimed to be effective for the PROX [32,33]. Later on, Oh and Sinkevitch compared various commercial catalysts for the PROX to be applied to fuel cell feed streams and reported that Ru/Al_2O_3 and Rh/Al_2O_3 were more selective than Pt/Al_2O_3 [34]. Since then, a number of catalysts more active for the CO oxidation than the H_2 oxidation have been reported, such as metal oxides (CoO_x, $CuO\text{-}CeO_2$), supported gold catalysts, and supported noble metal (Ru, Pt, and Rh) catalysts.

4.1. Metal oxides

A pair of transition metal and its oxide such as copper/copper oxide, silver/silver oxide, nickel/nickel oxide, and the higher and lower oxides of cerium has been claimed to be applied in PROX system [35]. CoO was reported to show the best performance among 3d transition metal oxides [36]. Supported cobalt oxide catalysts were also reported to be active for this reaction [37–40]. However, it was found that the CO methantion became dominant

Table 1
Comparison of the catalytic performance for the selective CO methanation reported in the literature

Catalyst	Preparation method	Feed composition	Temperature (K)	CO conversion (%)	Exit CO concentration (ppm)	Space velocity	Stability	Reference
0.5% Ru/Al_2O_3	Deposition-precipitation	0.3% CO, 16.7% CO_2, 15.0% H_2, 15.0% H_2O, and He balance	~430	96.57	103	500/h	n.d.	[24]
0.5% Rh/Al_2O_3	Deposition-precipitation	0.27% CO, 19.7% CO_2, and H_2 balance	~473	~95	n.d.	500/h	n.d.	[24]
0.5% $Ru/\alpha\text{-}Al_2O_3$	Commercial catalyst	0.3% CO, 20.0% CO_2, and H_2 balance	523	98.3	50	900/h	n.d.	[26]
35% Ni, 5% Al, 65% $Al_2O_3\text{-}H_2O$	Commercial catalyst	0.27% CO, 19.7% CO_2, and H_2 balance	473	98	60	900/h	n.d.	[26]
5% Ru/TiO_2	Impregnation	0.5% CO, 15.0% CO_2, 60.0% H_2, 0.8% H_2O, and He balance	493	n.d.	~20	2,525 ml/min/g_{cat}	n.d.	[27]
10% Ni/ZrO_2	Impregnation	0.5% CO, 15.0% CO_2, 60.0% H_2, 0.8% H_2O, and He balance	553	n.d.	~20	2,525 ml/min/g_{cat}	n.d.	[27]
3% Ru/Al_2O_3	Impregnation	0.9% CO, 24.5% CO_2, 68.9% H_2, 5.7% H_2O, and He balance	493	n.d.	~10	13,500/h	n.d.	[29]
$Re_2Y_9Ni_{89}O_x$	Sol–gel	2% CO, 14.9% CO_2, 63.3% H_2, and N_2 balance	≥513	~100	n.d.	1,250 ml/min/g_{cat}	n.d.	[30]

Table 2

Comparison of the catalytic performance over CuO-CeO_2 catalysts for the preferential CO oxidation reported in the literature

Catalyst	Preparation method	Feed composition	Temperature (K)	CO conversion (%)	Exit CO concentration (ppm)	Space velocity	Stability	Reference
20% CuO-CeO_2	Co-precipitation	1% CO, 1% O_2, 13.5% CO_2, 50% H_2, 20% H_2O, and He balance	438–448	~100	~10	250 ml/min/g_{cat}	Not stable	[44]
3% Cu-CeO_2	Impregnation	2% CO, 1% O_2, 70% H_2, and He balance	409	76.2	n.d.	1000/h	n.d.	[45]
$Cu_{0.1}Ce_{0.9}O_{2-y}$	Sol–gel	1% CO, 1.25% O_2, and H_2 balance	393	~80	n.d.	1000 ml/min/g_{cat}	Stable	[46]
$Cu_{0.15}Ce_{0.85}$	Urea nitrates combustion	1%CO, 1.25%O_2, 15%CO_2, 50%H_2, 10%H_2O, and He balance	463	99	n.d.	417 ml/min/g_{cat}	n.d.	[47]
15% Cu-CeO_2	Single-step citrate	0.03% CO, 0.03% O_2, 1% H_2, and He balance	473	98	n.d.	83,000/h	Not stable	[48]
5% CuO-CeO_2	Urea gelation/co-precipitation	1% CO, 1% O_2, 20% CO_2, 50% H_2, 10% H_2O, and He balance	438	99	n.d.	1333 ml/min/g_{cat}	n.d.	[49]
25% CuO-CeO_2	Citrate-hydrothermal	1% CO, 1.25% O_2, 15% CO_2, 50% H_2, 10% H_2O, and He balance	473–483	99	n.d.	417 ml/min/g_{cat}	Stable	[51]
$Ce_{0.8}Cu_{0.2}O_2$	Microemulsion	1% CO, 1.25% O_2, 50% H_2, and Ar balance	353–363	~100	n.d.	80,000/h	n.d.	[53]
Cu/CeO_2	Hydrothermal synthesis with cetyltrimethylammonium bromide	CO/O_2/H_2/H_2O/CO_2 (1/1/50/10/20)	393	97.3	n.d.	1.12 g_{cat} h/mol	Stable	[56]
5% Cu/Sm-CeO_2 (Sm:Ce = 1:9)	Impregnation/co-precipitation	1% CO, 2% O_2, and H_2 balance	423	~90	n.d.	2500 ml/min/g_{cat}	n.d.	[59]
$Cu_4Ce_{15.8}Co_{0.2}/\gamma\text{-}Al_2O_3$	Impregnation	1% CO, 1% O_2, 13% CO_2, 60% H_2, 10% H_2O, and He balance	483–493	~100	n.d.	60,000/h	n.d.	[60]
$Cu_{0.15}CeFe_{0.5}$	Urea nitrates combustion	1% CO, 1% O_2, 25% CO_2, 40% H_2, 10% H_2O, and He balance	448	~67	n.d.	500 ml/min/g_{cat}	n.d.	[65]
$Cu_5Ce_{47.5}Zr_{47.5}$	Co-precipitation	0.49% CO, 0.61% O_2, 2.08% CH_4, 23.26% CO_2, 26% H_2O, and H_2 balance	423	~100	n.d.	5000/h	Stable	[66]
5% CuO/20%CeO_2/γ-Al_2O_3	Impregnation	0.6% CO, 0.6% O_2, 30% H_2, and He balance	473	99	n.d.	300 ml/min/g_{cat}	Stable	[68]
7% CuO/$Ce_{0.9}Zr_{0.1}O_2$-Al_2O_3	Suspension/co-precipitation	1% CO, 1% O_2, 15% CO_2, 50% H_2, 10% H_2O, and He balance	433–443	~100	n.d.	167 ml/min/g_{cat}	Stable	[69]
4% Cu-CeO_2	Impregnation	0.5% CO, 0.5% O_2, 50% H_2, and N_2 balance	383	99.8	10	120 ml/min/g_{cat}	n.d.	[73]

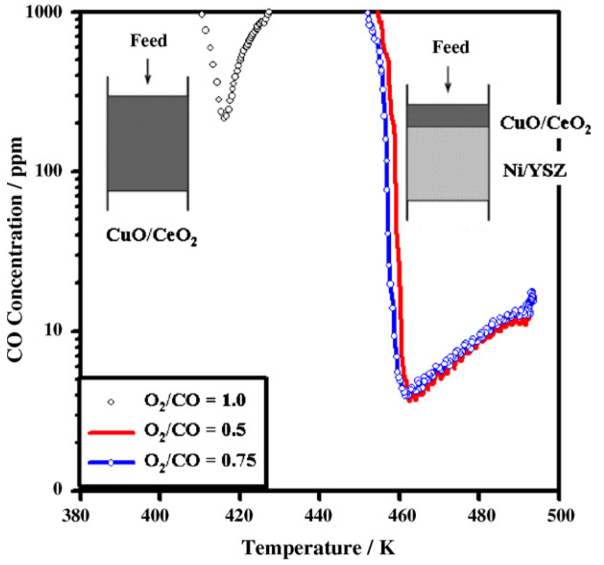

Fig. 3. The effluent concentrations of CO based on the dry gas composition after the preferential CO oxidation over the single bed ($CuO\text{-}CeO_2$) or the double bed system ($CuO\text{-}CeO_2$ and $Ni/Y\text{-}ZrO_2$) with increasing reaction temperatures at a ramping rate of 1 K/min. Reactants: 0.9% CO, 0.45 (0.68, 0.9) % O_2, 17.4% CO_2, 64. 6% H_2, 13.0% H_2O, balanced with N_2. F/W = 69 ml/min/g_{cat}.

in the presence of excess hydrogen over this catalyst [41]. Among mixed metal oxides, $CuO\text{-}CeO_2$ has been reported to be quite active and intensively studied by several groups [41–72]. The effect of preparation method [47–57], pretreatment condition [58], promoters [41,59–65], and support [66–69] on the PROX has been reported. Some $CuO\text{-}CeO_2$ catalysts for this reaction and their performance are summarized in Table 2. Most catalysts showed the narrow temperature window showing high CO conversions in the realistic condition. The exit CO concentration in ppm level has been seldom reported over this catalyst system. Its catalytic activity has been reported to be strongly dependent on the preparation methods including pretreatment conditions. For co-precipitated $CuO\text{-}CeO_2$ catalysts, the optimum calcinations temperature was determined to be 973 K [58]. Its surface area can be increased by adopting a citrate method, which accompanied the increase in the catalytic activity [48]. Although the addition of Co on $CuO\text{-}CeO_2/\gamma\text{-}Al_2O_3$ has been reported to have the positive effect on the catalytic activity [60–62], no promotional effect of noble metals such as Pt and Ru has been observed [41]. The reduction/oxidation processes of both copper and ceria have been accepted to be responsible for the high catalytic activity of $CuO\text{-}CeO_2$ catalysts. Therefore, the synthesis parameter inducing efficient mixing of Cu^{2+} and Ce^{4+} can give rise to the high PROX activity [51]. The importance of the interfacial positions between CuO and CeO_2 was also supported by DRIFTS and XANES study [72]. Based on the kinetic study, Caputa et al. reported that the reaction order in CO is variable with temperature ranging from values <1 up to 383 K and >1 at higher temperatures [73]. Some groups reported the gradual decrease in the activity with time on stream and proposed the different causes of deactivation such as accumulation of carbonate species [44], copper redistribution [46], and amassment of hydroxyl species as well as the sintering of copper species [70,71]. The presence of H_2O and CO_2 in the feed stream retarded their catalytic activity noticeably [41,44]. Furthermore, it was quite difficult to accomplish acceptable CO conversions over a wide reaction temperature in the practical condition. To overcome this weak point, the methanation reaction can be utilized after the PROX. Fig. 3 shows that the double-bed system composed of $CuO\text{-}CeO_2$ and $Ni/Y\text{-}ZrO_2$ can decrease the CO concentration from about 1 vol% to less than 10 ppm over a wide reaction temperature in the practical condition even in the presence of stoichiometric amounts of O_2 [74].

4.2. Supported gold catalysts

Supported gold catalysts have been reported to be quite active for the PROX especially at low temperatures [75]. However, the selectivity for CO oxidation over H_2 oxidation decreased rapidly with increasing reaction temperature. Kandoi et al. explained this observation based on the theoretical calculation [76]. They found that H oxidation (OH formation) competed with CO oxidation in PROX. The activation energy barrier for CO oxidation was calculated to be 0.18 eV on Au(1 1 1) and 0.96 eV on Pt(1 1 1), whereas the barrier for OH formation is 0.90 and 0.83 eV, respectively. The significantly weaker CO adsorption was calculated on Au at high temperature, which caused the substantial loss in the selectivity. Until now, Au/Mn_2O_3 [77], $Au/MO_x/Al_2O_3$ (M = Mg, Mn) [77–79], Au/CeO_2 [80–87], Au/Fe_2O_3 [88–91] and Au/TiO_2 [92–95,100] have been reported to be active for the PROX. Some supported gold catalysts for this reaction and their performance are summarized in Table 3. No supported gold catalyst has been reported to show stable activity to meet acceptable CO conversion over a long period of time in a realistic condition except the Au/Fe_2O_3 catalyst prepared using a two-stage calcinations to remove active sites for the water–gas shift reaction [90,91]. However, this catalyst exhibited narrow temperature window showing high CO conversions. Furthermore, the space velocity also strongly affects the PROX activity [90,91]. Recently, an aqueous phase PROX system mediated via polyoxometalates over supported gold catalysts has been proposed to be quite selective [101,102]. Because this reaction condition is quite different from the conventional case, further studies should be carried out to show its feasibility. The supported liquid-phase catalyst containing supported gold catalysts and a co-catalyst is claimed to remove high concentration of CO effectively at low temperatures [103].

4.3. Supported Pt-based catalysts

Since the conventional monometallic Pt catalyst has the noticeable PROX activity above 150 °C [107–111], the complete CO oxidation cannot be achieved at a low space velocity often encountered in the cyclic operation because of the reverse-water gas shift reaction. In the beginning, various zeolites were utilized as supports for Pt catalysts, such as A type zeolite [112–114], mordenite [115,116], and X type zeolite [115]. The catalyst material comprising an A type zeolite carrying at least one metal selected from the group consisting of Pt, Pd, Ru, Au, Rh and Ir, or an alloy of two or more metals was claimed for the PROX catalyst [117]. The Pt catalysts supported on zeolites such as NaY zeolite, NaX zeolite, Na mordenite, KL zeolite, NaZSM-5 zeolite and Naβ zeolite was also claimed for the PROX catalyst [118]. Recently, The Pt catalyst supported on a mesoporous silica such as FSM-16 showed the noticeable PROX activity at low temperatures [119,120]. Authors ascribed this enhanced activity to the electron-deficiency at the Pt surface due to the interaction with FSM-16. To increase catalytic activities at low temperatures, different methods have been tried for supported platinum catalysts. The pretreatment of Pt catalyst with water vapor was reported to reduce the metallic Pt particle size and enhance low-temperature catalytic activities for the PROX [121]. Various promoters have been investigated. A catalyst comprising Pt and at least one metal selected from the group consisting of Co, Ni, Cu, and Mn was claimed for the PROX catalyst [122]. Pt-Ru catalysts

Table 3

Comparison of the catalytic performance over supported gold catalysts for the preferential CO oxidation reported in the literature

Catalyst	Preparation method	Feed composition	Temperature (K)	CO conversion (%)	Exit CO concentration (ppm)	Space velocity	Stability	Reference
Au/MnO$_x$ (Au/Mn = 1/50)	Co-precipitation	1% CO, 1% O_2, and H_2 balance	323	~100	n.d.	10,000/h	Stable	[77]
5% Au/MnO$_x$/MgO/Al_2O_3 (Au:Mg:Mn = 1:5:5)	Homogeneous deposition-precipitation	1.14% CO, 0.57% O_2, 2.3% H_2, and He balance	~323	~93	n.d.	2500/h	n.d.	[78]
5% Au/MnO$_x$/MgO/Al_2O_3 (Au:Mg:Mn = 1:5:5)	Homogeneous deposition-precipitation	0.8% CO, 0.4% O_2, 70% H_2, and He balance	343	61	n.d.	2500/h	Stable	[79]
Au/CeO$_x$	Co-precipitation	1% CO, 1.5% O_2, 48% H_2, and He balance	393	~98	n.d.	120,000/h	Stable	[80]
2.5% Au/CeO_2	Deposition-precipitation	0.78% CO, 3.66% air, 72.06% H_2, 23.50% CO_2	423–473	n.d.	~100	624 ml/min/g_{cat}	n.d.	[81]
2.8% Au/CeO_2	Deposition-precipitation	0.8% CO, 0.4% O_2, 58.4% H_2, and He balance	333	~60	n.d.	2509 ml/min/g_{cat}	Stable	[82]
0.28AuCeGd	Urea gelation/co-precipitation	1% CO, 2.5% O_2, 15% CO_2, 50% H_2, 10% H_2O, and He balance	383	~100	n.d.	125 ml/min/g_{cat}	Stable	[83]
5.38% Au/FeO$_x$	Co-precipitation	1% CO, 1% O_2, 2% CO_2, 40% H_2, 2.6% H_2O, and He balance	323	~100	n.d.	500 ml/min/g_{cat}	Stable	[88]
5% Au/FeO_3	Co-precipitation	0.9% CO, 0.9% O_2, 50% H_2, 22% CO_2, 4.7% H_2O, and N_2 balance	353	99.8	n.d.	12,000/h	Stable	[90]
2% Au/TiO_2	Deposition-precipitation/gel combustion	1% CO, 2% O_2, 18% CO_2, 37% H_2, 5% H_2O, and He balance	353	n.d.	450	667 ml/min/g_{cat}	n.d.	[92]
3% Au/TiO_2	Deposition-precipitation	1% CO, 1% O_2, 50% H_2, and N_2 balance	283–323	~100	n.d.	2750 ml/min/g_{cat}	n.d.	[93]
1% Au/Ti/SBA-15	Deposition-precipitation/ impregnation	2% CO, 3% O_2, 10% H_2, and He balance	323	100	n.d.	2400/h	n.d.	[94]
0.38% Au/γ-Al_2O_3	Deposition-precipitation	1% CO, 0.5% O_2, 48% H_2, and He balance	373	~37	n.d.	4500 ml/min/g_{cat}	n.d.	[96]
2.7% Sm-3.5% Pb-2.4% V-2.6% Au/MgO	Urea precipitation	1% CO, 1% O_2, 58% H_2, and He balance	373	~85	n.d.	1000 ml/min/g_{cat}	n.d.	[97]
2% Au/ThO_2	Deposition-precipitation	1% CO, 1% O_2, 48% H_2, and Ar balance	333	~100	n.d.	6000/h	n.d.	[98]
1% Au/$Mn_{0.5}Ce_{0.5}O_2$	Deposition-precipitation/ impregnation	1.33% CO, 1.33% O_2, 65.33% H_2, and He balance	353	97.8	n.d.	30,000/h	n.d.	[99]
1% Pt-Au/CeO_2 (Pt:Au = 1:1)	Single-step sol-gel	1% CO, 1% O_2, 25% CO_2, 40% H_2, 10% H_2O, and He balance	403	58	n.d.	30,000/h	Stable	[104]
1.5% Au/ZnO	Co-precipitation	0.4% CO, 1% O_2, 20% CO_2, 70% H_2, and N_2 balance	313–393	~97	n.d.	3000/h	n.d.	[105]
1% Au-Pt/A zeolyte (Au:Pt = 1:2)	Co-impregnation	1% CO, 1% O_2, 10% CO_2, 40% H_2, 10% H_2O, and He balance	463	~100	n.d.	500 ml/min/g_{cat}	n.d.	[106]

Table 4

Comparison of the catalytic performance over supported Pt catalysts for the preferential CO oxidation reported in the literature

Catalyst	Preparation method	Feed composition	Temperature (K)	CO conversion (%)	Exit CO concentration (ppm)	Space velocity	Stability	Reference
0.5% Pt/Al_2O_3	Commercial catalyst	0.09% CO, 0.08% O_2, 0.85% H_2, and N_2 balance	473	~97	n.d.	20,000/h	n.d.	[34]
1% Pt/Al_2O_3 monolith	Impregnation	1% CO, 1% O_2, 19% CO_2, 38.39% H_2, 17% H_2O, and N_2 balance	433	~100	n.d.	12,000/h	Stable	[108]
5% Pt/γ-Al_2O_3	Impregnation	1% CO, 1% O_2, and H_2 balance	423–473	~100	n.d.	1000 ml/min/g_{cat}	n.d.	[121]
0.5% Pt/Al_2O_3	Commercial catalyst	1% CO, 1% O_2, 75% H_2, and N_2 balance	498	~82	n.d.	1200 ml/min/g_{cat}	n.d.	[109]
1% Pt/3A	Impregnation	0.5% CO, 1% O_2, 18% CO_2, 37% H_2, 5% H_2O, and He balance	453–493	~100	n.d.	67,000/h	n.d.	[114]
6% Pt-mordenite	Ion-exchange	1% CO, 1% O_2, 20% H_2O, and H_2 balance	473	~70	n.d.	1000 ml/min/g_{cat}	Stable	[115]
1% Pt-mordenaite	Impregnation	1% CO, 1.5% O_2, 40% H_2, 20% CO_2, and N_2 balance	393–453	n.d.	≤10	10,000/h	n.d.	[116]
5% Pt/FSM-16	Impregnation	1% CO, 0.5% O_2, 5% N_2, and H_2 balance	333–423	~100	n.d.	200 ml/min/g_{cat}	Not stable	[120]
Pt-Ru/Al_2O_3	Impregnation	1% CO, 2% O_2, 17% CO_2, 36% H_2, 17% H_2O, and N_2 balance	373	~100	n.d.	667 ml/min/g_{cat}	n.d.	[123]
1% Pt-1% Ru/SiO_2	Co-impregnation	0.5% CO, 0.5% O_2, 45% H_2, and N_2 balance	393–433	~100	n.d.	2000 ml/min/g_{cat}	n.d.	[124]
1% Pt-3% Sn/Al_2O_3	Sol–gel	1% CO, 1% O_2, 58% H_2, 25% CO_2, 10% H_2O, and He balance	383	99.5	n.d.	400 ml/min/g_{cat}	Stable	[127]
Pt-Fe/mordenaite (Pt:Fe = 2:1)	Ion-exchange	1% CO, 0.5% O_2, 20% H_2O, 25% CO_2, and H_2 balance	353–473	100	n.d.	2000 ml/min/g_{cat}	n.d.	[130]
4% Pt-0.5% Fe/Mordenaite	Ion-exchange	1% CO, 0.5% O_2, and H_2 balance	323	~90	n.d.	50,000/h	n.d.	[132]
FeO_x/1% Pt/CeO_x	Impregnation	1.5% CO, 3% O_2, 20% H_2, and N_2 balance	333	~98	n.d.	66.7 ml/min/g_{cat}	n.d.	[134]
$FeO_x/Pt/TiO_2$ (Fe:Pt = 350:1)	Impregnation	3% CO, 1.8% O_2, 75% H_2, 3.5% H_2O, and N_2 balance	353	~80	n.d.	15,000/h	n.d.	[135]
1% Pt-0.11% Fe/SiO_2	Co-impregnation	0.5% CO, 0.5% O_2, 45% H_2, and N_2 balance	433	~ 96	n.d.	2000 ml/min/g_{cat}	Not stable	[137]
5% Pt-5% Ce/γ-Al_2O_3	Co-impregnation	1% CO, 1% O_2, and H_2 balance	423	~95	n.d.	1000 ml/min/g_{cat}	n.d.	[140]
1% Pt-1% Ce/γ-Al_2O_3	Co-impregnation	1% CO, 1% O_2, 10.09% CO_2, 2.3% H_2O, and H_2 balance	473	~100	n.d.	1000 ml/min/g_{cat}	n.d.	[141]
1% Pt-1% CeO_x/activated carbon	Impregnation	1% CO, 1% O_2, 60% H_2, 15% CO_2, 10% H_2O, and He balance	423	~100	n.d.	400 ml/min/g_{cat}	Stable	[142]
1% Pt/15% Mn/Al_2O_3	Impregnation	1% CO, 1% O_2, 60% H_2, 5% CO_2, 5% H_2O, and He balance	453	~90	n.d.	12,000/h	Stable	[143]
0.5% Pt-Co/YSZ (Co/Pt = 10)	Impregnation	0.9% CO, 0.9% O_2, 64.6% H_2, 17.4% CO_2, 13% H_2O, and N_2 balance	380–423	n.d.	≤10	278 ml/min/g_{cat}	Stable	[149]
3.32% Co/1.44% Pt/TiO_2	Impregnation	1% CO, 1.25% O_2, 7% H_2O, 18% CO_2, and H_2 balance	293	~96	n.d.	22,000/h	Not stable	[152]
1.4% Pt-1.25% Co-1.25% Ce/Al_2O_3	Co-impregnation	1% CO, 1% O_2, 60% H_2, 25% CO_2, 10% H_2O, and He balance	383	~100	n.d.	400 ml/min/g_{cat}	stable	[150]
1.4% Pt-1.25% Co-1.25% Ce/MgO	Impregnation	1% CO, 1% O_2, 60% H_2, 25% CO_2, 10% H_2O, and He balance	423	~100	n.d.	400 ml/min/g_{cat}	n.d.	[151]
1% Pt-1.5% Ni/γ-Al_2O_3	Impregnation	1% CO, 1% O_2, 50% H_2, 20% CO_2, 2% H_2O, and He balance	403	~99	n.d.	1000 ml/min/g_{cat}	n.d.	[153]
1% Pt/5% Nb-Al_2O_3	Co-precipitation	0.8% CO, 0.8% O_2, 51% H_2, and He balance	423	~100	n.d.	975 ml/min/g_{cat}	n.d.	[154]
K-Pt/Al_2O_3	Impregnation	0.2% CO, 0.2% O_2, 75% H_2, 5% H_2O, and He balance	403	~100	n.d.	30,000/h	n.d.	[157]
2% Pt-3% Mg/Al_2O_3	Impregnation	1% CO, 0.75% O_2, 65% H_2, 20% CO_2, 10% H_2O, and N_2 balance	443	87.9	n.d.	60,000/h	n.d.	[155]
(2.0% Na) 1% Pt-1.8% Co/Al_2O_3	Impregnation	0.1% CO, 0.1% O_2, 1% H_2, and N_2 balance	373	n.d.	~0	25,000/h	n.d.	[156]
1% Pt/$Ce_{0.8}Zr_{0.2}O_2$	Impregnation/ co-precipitation	5% CO, 2.5% O_2, and H_2 balance	333	~80	n.d.	280 ml/h/g_{cat}	Stable	[161]
1% Pt-7% Pd/CeO_2	Co-impregnation/sol-gel	1% CO, 1% O_2, 40% H_2, 25% CO_2, 10% H_2O, and He balance	363	~84	n.d.	500 ml/min/g_{cat}	n.d.	[168]
Pt/CeO_2	Impregnation	1% CO, 1% O_2, 60% H_2, 5% CO_2, 5% H_2O, and He balance	373	~100	n.d.	12,000/h	n.d.	[163]
1% Pt/CeO_2	Impregnation	1% CO, 0.5% O_2, and H_2 balance	383	65	n.d.	1220 ml/min/g_{cat}	n.d.	[164]

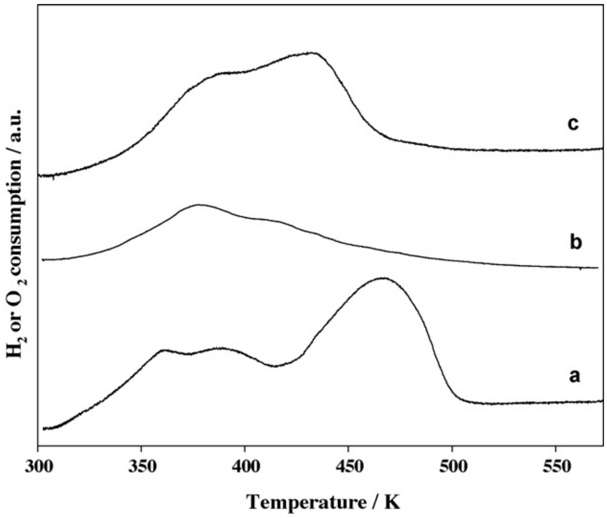

Fig. 4. The temperature programmed reduction (TPR) pattern of Pt-Co/YSZ containing 1 wt% Pt and 1.5 wt.% Co calcined at 573 K, the temperature programmed oxidation of the same catalyst after the TPR experiment (b) and the TPR pattern of the same catalyst after the TPO experiment (c).

supported on alumina [123], SiO_2 [124], and mordenite [125] were reported to be superior to the monometallic Pt catalyst. Several groups have reported that the PROX at low temperatures could be enhanced by the addition of 2nd metals such as Sn [126,127], Fe [128–139], Ce [140–142], Mn [143,144], Co [144–152], Ni [144,153], Nb [154], and alkali metals [155–160]. Pt catalysts supported on $CeZrO_x$ [161,162] and CeO_2 [163–168] were also reported to be active for this reaction. Some supported Pt catalysts for this reaction and their performance are summarized in Table 4. Although lots of works have been conducted over Pt-based catalysts compared with other PROX catalysts, only a few catalysts have been reported to show a wide temperature window showing the acceptable CO conversion in a realistic condition over a long period of time.

Until now, several catalyst systems have been characterized to reveal their superior catalytic activity to the conventional monometallic Pt catalysts. The carbon-supported Pt_3Sn catalyst has the lower activation energy for CO oxidation than that for H_2 oxidation, while Pt/Al_2O_3 catalyst has the similar activation energy for both reactions which are larger than those of Pt_3Sn catalysts [126]. The mechanistic model involving separation of the CO or H_2 adsorption sites (Pt sites) and oxygen adsorption sites (Sn sites and SnO_x islands adjacent to the active PtSn particles) was also proposed [126]. The enhanced PROX activity over Fe-oxide promoted Pt/alumina catalyst was also explained with a dual site non-competitive mechanism for CO oxidation similarly to that of Pt_3Sn catalyst [129]. In addition, it was suggested that the electronic states of the Pt metal particles could be changed by the Fe oxide [129]. In the case of Pt-Fe/zeolite catalysts, CO coverage and CO bond strength on Pt were observed to be extremely lowered by the combination with Fe [130]. In a separate work, reoxidation of Fe was proposed to be a significant cause of the loss of activity of $PtFe/\gamma\text{-}Al_2O_3$ catalyst [131]. The promotional effect of Mg was ascribed to an increase in the hydroxyl groups as well as to an increase in the electron density on the surface of the Pt catalyst [155]. The incorporation of sodium with alumina inhibits the formation of the surface spinel cobalt species and promotes the formation of the Pt-Co bimetallic interphase [156].

Recently, $Pt\text{-}Co/Y\text{-}ZrO_2$ has been proposed to be one of active PROX catalysts after a careful pretreatment [149]. This catalyst can reduce the CO concentration to below 10 ppm in the temperature range 380–423 K in the practical condition. The isolated bimetallic Pt-Co nanoparticles interacting with the support was observed. As shown in Fig. 4, the O_2 consumption is observed in the temperature range 300–450 K over reduced Pt-Co/YSZ. This oxidized catalyst can be reduced again in the almost same temperature region. From this result, the reduced Co in the bimetallic Pt-Co phase can be oxidized with O_2 and reduced again with H_2. This is consistent with the previous XAFS result that part of the Pt–Co bonds disappear while an oxidation of Pt is observed when it was exposed to air [169]. Based on these results, the reaction scheme can be proposed as shown in Fig. 5. A dual site non-competitive mechanism is valid and the role of reduced M (M = Ni or Co) is to activate O_2. The oxidized M can be reduced by H_2, which can be facilitated in the presence of Pt metal.

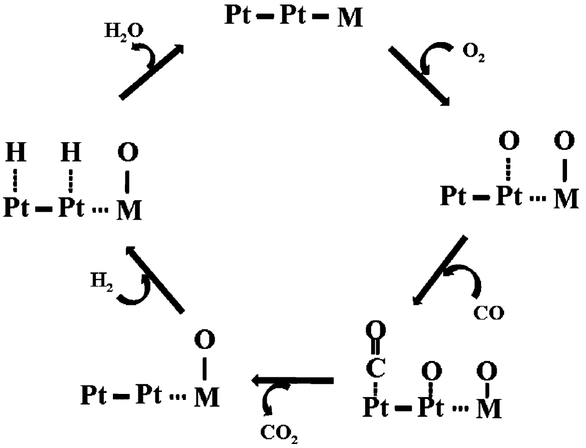

Fig. 5. The reaction scheme for the preferential CO oxidation over supported Pt-M (M = Co or Ni) catalysts.

4.4. Supported Ru, Rh, and Ir catalysts

Supported Ru catalysts have been actively applied to the PROX system since Oh and Sinkevitch reported that Ru/Al_2O_3 was the most active among commercial catalysts [34]. The catalyst comprising Ru supported on an alumina hydrate was claimed for the PROX catalyst [170]. The supported Ru catalyst has been reported to be affected noticeably by the preparation parameters such as Ru precursors, reducing agents, and pretreatment conditions [171–174]. The combination of a direct hydrogen treatment and use of a nitrate precursor resulted in the finely dispersed Ru catalysts highly active for PROX [171]. The Ru/Al_2O_3 catalyst prepared by the liquid-phase reduction showed the best performance after reduction at 523 K [172–174]. The close relation between the low-temperature PROX activity and the ratio of Ru(0) was revealed by XPS study [173]. Until now, this Ru/Al_2O_3 catalyst can be considered to be the most promising based on the real operation data [175–178]. However, there has been no report that the acceptable CO removal can be achieved with the high inlet CO concentration such as around 1 vol% in the real gas composition.

Supported Ru catalysts have also some advantages over other supported noble metal catalysts because both oxidation and hydrogenation can be accomplished at once. This can provide the extended the temperature range to achieve the acceptable CO removal [174,179]. Compared with supported Ru catalysts, supported Rh and Ir catalysts have been reported to be less selective for the PROX. Some supported Ru, Rh, and Ir catalysts for this reaction and their performance are summarized in Table 5.

Table 5
Comparison of the catalytic performance of supported Ru, Rh, and Ir catalysts for the preferential CO oxidation reported in the literature

Catalyst	Preparation method	Feed composition	Temperature (K)	CO conversion (%)	Exit CO concentration (ppm)	Space velocity	Stability	Reference
0.5% Ru/Al_2O_3	Commercial catalyst	0.09% CO, 0.08% O_2, 0.85% H_2, and N_2 balance	393	~100	n.d.	20,000/h	n.d.	[34]
1% Ru/SiO_2	Impregnation	0.5% CO, 0.5% O_2, 45% H_2, 15% CO_2, 10% H_2O, and N_2 balance	393–443	n.d.	≤30	2000 ml/min/g_{cat}	n.d.	[171]
1% Ru/Al_2O_3	Impregnation	0.5% CO, 0.75% O_2, 3% N_2, 20% CO_2, 11% H_2O, and H_2 balance	373–433	n.d.	≤10	7500/h (dry base)	Stable	[176]
0.5% Ru/Al_2O_3	Commercial catalyst	0.5% CO, 1% O_2, 37% H_2, 18% CO_2, 5% H_2O, and He balance	393–453	~100	n.d.	67,000/h	n.d.	[178]
0.5% Rh/Al_2O_3	Commercial catalyst	0.09% CO, 0.08% O_2, 0.85% H_2, and N_2 balance	393	~100	n.d.	20,000/h	n.d.	[34]
1% Rh/zeolite 3A	Impregnation	1% CO, 2% O_2, 37% H_2, 18% CO_2, 5% H_2O, and He balance	353–373	n.d.	≤10	660 ml/min/g_{cat}	n.d.	[180]
0.5% Rh/Nb_2O_5	Impregnation/precipitation	0.2% CO, 1% O_2, 3% H_2, and He balance	373	~100	n.d.	1000 ml/min/g_{cat}	n.d.	[181]
K_2CO_3-Rh/SiO_2 (K/Rh = 3)	Impregnation	0.2% CO, 0.2% O_2, 75% H_2, and He balance	403	~100	n.d.	4000 ml/min/g_{cat}	n.d.	[182]
$Ir/FeO_x/Al_2O_3$ (Fe/Ir = 5)	Impregnation	2% CO, 1% O_2, 40% H_2, and He balance	353	74	n.d.	40,000/h	n.d.	[183]
Ir/CeO_2	Homogeneous deposition-precipitation	2% CO, 1% O_2, 40% H_2, and He balance	353	~70	n.d.	667 ml/min/g_{cat}	n.d.	[184]

5. Summary and outlook

Two different approaches such as hydrogen separation through the selective diffusion and catalytic purification to remove CO in a H_2-rich stream for the PEMFC were compared and discussed on their characteristics. In the case of membrane separation, the thin layer of Pd-based alloy metal on the porous ceramic material coupled with the catalytic purification is the most advanced method at present. The development of non-palladium-based membranes that offer a lower cost, high flux, and high durability is quite plausible in the future.

Due to the intensive works during last decades, supported Ru catalysts and Pt-based alloy catalysts have been successfully developed. However, the PROX catalysts which can selectively remove high concentrations of CO above 1 vol% can contribute to reduce the size of fuel processor by minimizing the water–gas shift reactor. The combination of highly selective PROX catalysts and the CO methanation catalyst can provide the extended temperature range to achieve the acceptable CO removal. During this research on the catalytic purification, the progress on the membrane operating at relatively high temperatures [185–188] or the CO-tolerant anode [189] should be carefully kept eye on not to be superfluous.

Acknowledgement

We acknowledge financial support from the Samsung Advanced Institute of Technology (SAIT).

References

[1] B.C.H. Steele, A. Heinzel, Nature 414 (2001) 345.
[2] C. Song, Catal. Today 77 (2002) 17.
[3] R. Farrauto, S. Hwang, L. Shore, W. Ruettinger, J. Lampert, T. Giroux, Y. Liu, O. Ilinich, Annu. Rev. Mater. Res. 33 (2003) 1.
[4] A.F. Ghenciu, Curr. Opin. Solid State Mater. Sci. 6 (2002) 389.
[5] M. Krumpelt, T.R. Krause, J.D. Carter, J.P. Kopasz, S. Ahmed, Catal. Today 77 (2002) 3.
[6] S. Ahmed, M. Krumpelt, Int. J. Hydrogen Energy 26 (2001) 291.
[7] J.R. Rostrup-Nielsen, K. Aasberg-Petersen, in: W. Vielstich, A. Lamm, H.A. Gasteiger (Eds.), Handbook of Fuel Cells: Fundamentals Technology and Applications, vol. 3, John Wiley & Sons Ltd., West Sussex, 2003, , p. 190part 2.
[8] J.R. Ladebeck, J.P. Wagner, in: W. Vielstich, A. Lamm, H.A. Gasteiger (Eds.), Handbook of Fuel Cells: Fundamentals Technology and Applications, vol. 3, John Wiley & Sons Ltd., West Sussex, 2003, , p. 190part 2.
[9] F. Marschner, F.W. Moeller, in: B.E. Leach (Ed.), Applied Industrial Catalysis, vol. 2, Academic Press, New York, 1983, p. 215.
[10] D.L. Trimm, Appl. Catal. A: Gen. 296 (2005) 1.
[11] H.P. Dhar, L.G. Christner, A.K. Kush, J. Electrochem. Soc. 134 (12) (1987) 3021.
[12] L. Shore, R.J. Farrauto, in: W. Vielstich, A. Lamm, H.A. Gasteiger (Eds.), Handbook of Fuel Cells: Fundamentals Technology and Applications, vol. 3, John Wiley & Sons Ltd., West Sussex, 2003, , p. 211part 2.
[13] G.Q. Lu, J.C. Diniz da Costa, M. Duke, S. Giessler, R. Socolow, R.H. Williams, T. Kreutz, J. Colloid Interf. Sci. 314 (2007) 589.
[14] N.W. Ockwig, T.M. Nenoff, Chem. Rev. 107 (2007) 4078.
[15] G.J. Grashoff, C.E. Pilkington, C.W. Corti, Plat. Met. Rev. 27 (1983) 157.
[16] F.A. Lewis, K. Kandasamy, B. Baranowski, Plat. Met. Rev. 32 (1988) 22.
[17] J. Shu, B.P.A. Grandjean, A. Van Neste, S. Kaliaguine, Can. J. Chem. Eng. 69 (1991) 1036.
[18] E. Kikuchi, Catal. Today 56 (2000) 97.
[19] T.M. Adams, J. Mickalonis, Mater. Lett. 61 (2007) 817.
[20] M.L. Doyle, N. Edwards, U.S. Patent No. 6,350,297 (2002).
[21] S. Wieland, T. Melin, in: W. Vielstich, A. Lamm, H.A. Gasteiger (Eds.), Handbook of Fuel Cells: Fundamentals Technology and Applications, vol. 3, John Wiley & Sons Ltd., West Sussex, 2003, , p. 202part 2.
[22] W.H. Wang, D. Dong, C.H. Shek, Mater. Sci. Eng. R 44 (2004) 45.
[23] M.D. Dolan, N.C. Dave, A.Y. Ilyushechkin, L.D. Morpeth, K.G. McLennan, J. Membr. Sci. 285 (2006) 30.
[24] B.S. Baker, J. Huebler, H.R. Linden, J. Meek, U.S. Patent No. 3,615,164 (1971).
[25] G. Böhm, T. Staneff, J. Steinwandel, U.S. Patent No. 5,904,913 (1997).
[26] A. Rehmat, S.S. Randhava, Ind. Eng. Chem. Prod. Res. Dev. 9 (1970) 512.
[27] S. Takenaka, T. Shimizu, K. Otsuka, Int. J. Hydrogen Energ. 29 (2004) 1065.
[28] M. Echigo, T. Tabata, J. Chem. Eng. Jpn. 37 (2004) 75.
[29] R.A. Dagle, Y. Wang, G.-G. Xia, J.J. Strohm, J. Holladay, D.R. Palo, Appl. Catal. A: Gen. 326 (2007) 213.

[30] M. Krämer, M. Duisberg, K. Stöwe, W.F. Maier, J. Catal. 251 (2007) 410.
[31] M.L. Brown Jr., A.W. Green, G. Cohn, H.C. Andersen, Ind. Eng. Chem. 52 (1960) 841.
[32] J.G.E. Cohn, U.S. Patent No. 3,216,783 (1965).
[33] J.G.E. Cohn, U.S. Patent No. 3,631,073 (1965).
[34] S.H. Oh, R.M. Sinkevitch, J. Catal. 142 (1993) 254.
[35] J.A. Cole, R.K. Lyon, U.S. Patent No. 6,475,454 (2002).
[36] Y. Teng, H. Sakurai, A. Ueda, T. Kobaysahi, Int. J. Hydrogen Energ. 24 (1999) 355.
[37] K. Omata, Y. Kobayashi, M. Yamada, Catal. Commun. 8 (2007) 1.
[38] K. Omata, Y. Kobayashi, M. Yamada, Catal. Today 117 (2006) 311.
[39] G. Qiang, W. Meiling, L. Yuan, B. Xue, Chin. J. Catal. 28 (2007) 953.
[40] M.M. Yung, Z. Zhao, M.P. Woods, U.S. Ozkan, J. Mol. Catal. A-Chem. 279 (2008) 1.
[41] E.-Y. Ko, E.D. Park, K.W. Seo, H.C. Lee, D. Lee, S. Kim, Catal. Today 116 (2006) 377.
[42] G. Avogouropolos, T. Ioannides, H.K. Matralis, J. Batista, S. Hocevar, Catal. Lett. 73 (2001) 33.
[43] J.B. Wang, W.-H. Shih, T.-J. Huang, Appl. Catal. A: Gen. 203 (2000) 191.
[44] D.H. Kim, J.E. Cha, Catal. Lett. 86 (2003) 107.
[45] F. Marino, C. Descorme, D. Duprez, Appl. Catal. B: Environ. 58 (2005) 175.
[46] G. Sedmak, S. Hocevar, J. Levec, J. Catal. 213 (2003) 135.
[47] G. Avogouropolos, T. Ioannides, H.K. Matralis, Appl. Catal. B: Environ. 56 (2005) 87.
[48] G. Marban, A.B. Fuertes, Appl. Catal. B: Environ. 57 (2005) 43.
[49] Y. Liu, Q. Fu, M.F. Stephanopoulos, Catal. Today 93–95 (2004) 241.
[50] C.M. Bae, J.B. Ko, D.H. Kim, Catal. Commun. 6 (2005) 507.
[51] G. Avgouropoulos, T. Ioannides, Appl. Catal. B: Environ. 67 (2006) 1.
[52] H.C. Lee, D.H. Kim, Catal. Today 132 (2008) 109.
[53] D. Gamarra, G. Munuera, A.B. Hungría, M. Fernández-García, J.C. Conesa, P.A. Midgley, X.Q. Wang, J.C. Hanson, J.A. Rodríguez, A. Martínez-Arias, J. Phys. Chem. C 111 (2007) 11026.
[54] G. Avgouropoulos, T. Ioannides, Appl. Catal. A: Gen. 244 (2003) 155.
[55] Z. Liu, R. Zhou, X. Zheng, J. Mol. Catal. A-Chem. 255 (2006) 103.
[56] M. Tada, R. Bal, X. Mu, R. Coquet, S. Namba, Y. Iwasawa, Chem. Commun. (2007) 4689.
[57] D. Gamarra, A. Hornés, Zs. Koppány, Z. Schay, G. Munuera, J. Soria, A. Martínez-Arias, J. Power Sources 169 (2007) 110.
[58] C.R. Jung, J. Han, S.W. Nam, T.-H. Lim, S.-A. Hong, H.-I. Lee, Catal. Today 93–95 (2004) 183.
[59] J.B. Wang, S.-C. Lin, T.-J. Huang, Appl. Catal. A: Gen. 232 (2002) 107.
[60] J.-W. Park, J.-H. Jeong, W.-L. Yoon, H. Jung, H.-T. Lee, D.-K. Lee, Y.-K. Park, Y.-W. Rhee, Appl. Catal. A: Gen. 274 (2004) 25.
[61] J.W. Park, J.H. Jeong, W.L. Yoon, C.S. Kim, D.-K. Lee, Y.-K. Park, Y.W. Rhee, Int. J. Hydrogen Energ. 30 (2005) 209.
[62] J.W. Park, J.H. Jeong, W.L. Yoon, Y.W. Rhee, J. Power Sources 132 (2004) 18.
[63] P.K. Cheekatamarla, W.S. Epling, A.M. Lane, J. Power Sources 147 (2005) 178.
[64] A. Martinez-Arias, A.B. Hungria, M. Fernández-García, J.C. Conesa, G. Munuera, J. Power Sources 151 (2005) 32.
[65] K. Sirichaiprasert, A. Luengnaruemitchai, S. Pongstabodee, Int. J. Hydrogen Energ. 32 (2007) 915.
[66] P. Ratnasamy, D. Srinivas, C.V.V. Satyanarayana, P. Manikandan, R.S. Senthil Kumaran, M. Sachin, V.N. Shetti, J. Catal. 221 (2004) 455.
[67] R. Lin, M.-F. Luo, Y.-J. Zhong, Z.-L. Yan, G.-Y. Liu, W.-P. Liu, Appl. Catal. A: Gen. 255 (2003) 331.
[68] E. Moretti, M. Lenarda, L. Storaro, A. Talon, R. Frattini, S. Polizzi, E. Rodríguez-Castellón, A. Jiménez-López, Appl. Catal. B: Environ. 72 (2007) 149.
[69] Y.-Z. Chen, B.-J. Liaw, W.-C. Chang, C.-T. Huang, Int. J. Hydrogen Energ. 32 (2007) 4550.
[70] H. Zou, X. Dong, W. Lin, Appl. Surf. Sci. 253 (2006) 2893.
[71] A. Martinez-Arias, A.B. Hungria, G. Munuera, D. Gamarra, Appl. Catal. B: Environ. 65 (2006) 207.
[72] D. Gamarra, C. Belver, M. Fernández-García, A. Martínez-Arias, J. Am. Chem. Soc. 129 (2007) 12064.
[73] T. Caputo, L. Lisi, R. Pirone, G. Russo, Ind. Eng. Chem. Res. 46 (2007) 6793.
[74] Y.H. Kim, E.D. Park, H.C. Lee, K.H. Lee, S. Kim, Stud. Surf. Sci. Catal. 167 (2007) 171.
[75] G.C. Bond, C. Louis, D.T. Thompson, Catalysis by Gold, Imperial College Press, London, 2006.
[76] S. Kandoi, A.A. Gokhale, L.C. Grabow, J.A. Dumesic, M. Mavrikakis, Catal. Lett. 93 (2004) 93.
[77] R.M.T. Sanchez, A. Ueda, K. Tanaka, M. Haruta, J. Catal. 168 (1997) 125.
[78] R.J.H. Grisel, B.E. Nieuwenhuys, J. Catal. 199 (2001) 48.
[79] R.J.H. Grisel, C.J. Weststrate, A. Goossens, M.W.J. Craje, A.M. van der Kraan, B.E. Nieuwenhuys, Catal. Today 72 (2002) 123.
[80] G. Panzera, V. Modafferi, S. Candamano, A. Donato, F. Frusteri, P.L. Antonucci, J. Power Sources 135 (2004) 177.
[81] W.-S. Shin, C.-R. Jung, J. Han, S.-W. Nam, T.-H. Lim, S.-A. Hong, H.-I. Lee, J. Ind. Eng. Chem. 10 (2004) 302.
[82] S. Carrettin, P. Concepcion, A. Corma, J.M.L. Nieto, V.F. Puntes, Angew. Chem. Int. Ed. 43 (2004) 2538.
[83] W. Deng, J.D. Jesus, H. Saltsburg, M. Flytzani-Stephanopoulos, Appl. Catal. A: Gen. 291 (2005) 126.
[84] E.-Y. Ko, E.D. Park, H.C. Lee, D. Lee, S. Kim, Solid State Phenom. 124–126 (2007) 1749.
[85] F. Arena, P. Famulari, G. Trunfio, G. Bonura, F. Frusteri, L. Spadaro, Appl. Catal. B: Environ. 66 (2006) 81.
[86] A. Jain, X. Zhao, S. Kjergaard, S.M. Stagg-Williams, Catal. Lett. 104 (2005) 191.
[87] J. Guzman, S. Carrettin, A. Corma, J. Am. Chem. Soc. 127 (2005) 3286.
[88] A. Luengnaruemitchai, D.T.K. Thoa, S. Osuwan, E. Gulari, Int. J. Hydrogen Energ. 30 (2005) 981.
[89] M.J. Kahlich, H.A. Gasteiger, R.J. Behm, J. Catal. 182 (1999) 430.
[90] P. Landon, J. Ferguson, B.E. Solsona, T. Garcia, A.F. Carley, A.A. Herzing, C.J. Kiely, S.E. Golunski, G.J. Hutchings, Chem. Commun. 27 (2005) 3385.
[91] P. Landon, J. Ferguson, B.E. Solsona, T. Garcia, S. Al-Sayari, A.F. Carley, A.A. Herzing, C.J. Kiely, M. Makkee, J.A. Moulijn, A. Overweg, S.E. Golunski, G.J. Hutchings, J. Mater. Chem. 16 (2006) 199.
[92] C. Galletti, S. Fiorot, S. Specchia, G. Saracco, V. Specchia, Chem. Eng. J. 134 (2007) 45.
[93] W.-Y. Yu, W.-S. Lee, C.-P. Yang, B.-Z. Wan, J. Chin. Inst. Chem. Eng. 38 (2007) 151.
[94] M. Ruszel, B. Grzybowska, M. Łaniecki, M. Wójtowski, Catal. Commun. 8 (2007) 1284.
[95] J. Steyn, G. Pattrick, M.S. Scurrell, D. Hildebrandt, M.C. Raphulu, E. van der Lingen, Catal. Today 122 (2007) 254.
[96] G.K. Bethke, H.H. Kung, Appl. Catal. A: Gen. 194–195 (2000) 43.
[97] A. Tompos, M. Hegedüs, J.L. Margitfalvi, E.G. Szabó, L. Végvári, Appl. Catal. A: Gen. 334 (2008) 348.
[98] T. Tabakova, V. Idakiev, K. Tenchev, F. Boccuzzi, M. Manzoli, A. Chiorino, Appl. Catal. B: Environ. 63 (2006) 94.
[99] L.-H. Chang, N. Sasirekha, Y.-W. Chen, W.-J. Wang, Ind. Eng. Chem. Res. 45 (2006) 4927.
[100] M. Manzoli, F. Vindigni, A. Chiorino, T. Tabakova, V. Idakiev, F. Boccuzzi, React. Kinet. Catal. Lett. 91 (2007) 213.
[101] W.B. Kim, T. Voitl, G.J. Rodriguez-Rivera, S.T. Evans, J.A. Dumesic, Angew. Chem. Int. Ed. 44 (2005) 778.
[102] W.B. Kim, G.J. Rodriguez-Rivera, S.T. Evans, T. Voitl, J.J. Einspahr, P.M. Voyles, J.A. Dumesic, J. Catal. 235 (2005) 327.
[103] H.C. Lee, S. Kim, Y. Potapova, E.D. Park, E.-Y. Ko, U.S. Patent Application 0,165,576.
[104] S. Monyanon, S. Pongstabodee, A. Luengnaruemitchai, J. Power Sources 163 (2006) 547.
[105] Y.H. Wang, J.L. Zhu, J.C. Zhang, L.F. Song, J.Y. Hu, S.L. Ong, W.J. Ng, J. Power Sources 155 (2006) 440.
[106] P. Naknam, A. Luengnaruemitchai, S. Wongkasemjit, S. Osuwan, J. Power Sources 165 (2007) 353.
[107] A. Manasilp, E. Gulari, Appl. Catal. B: Environ. 37 (2002) 17.
[108] S. Zhou, Z. Yuan, S. Wang, Int. J. Hydrogen Energ. 31 (2006) 924.
[109] M.J. Kahlich, H.A. Gasteiger, R.J. Behm, J. Catal. 171 (1997) 93.
[110] B. Atalik, D. Uner, J. Catal. 241 (2006) 268.
[111] O.S. Alexeev, S.Y. Chin, M.H. Engelhard, L. Ortiz-Soto, M.D. Amiridis, J. Phys. Chem. B 109 (2005) 23430.
[112] M. Watanabe, H. Uchida, H. Igarashi, M. Suzuki, Chem. Lett. (1995) 21.
[113] I. Rosso, C. Galletti, S. Fiorot, G. Saracco, E. Garrone, V. Specchia, J. Porous Mat. 14 (2007) 245.
[114] I. Rosso, C. Galletti, G. Saracco, E. Garrone, V. Specchia, Appl. Catal. B: Environ. 48 (2004) 195.
[115] H. Igarashi, H. Uchida, M. Suzuki, Y. Sasaki, M. Watanabe, Appl. Catal. A: Gen. 159 (1997) 159.
[116] S. Ren, X. Hong, Fuel Process. Technol. 88 (2007) 383.
[117] E. Yasumoto, K. Hatoh, T. Gamou, U.S. Patent No. 5,702,838 (1997).
[118] R. Andorf, W. Maunz, C. Plog, T. Stengel, U.S. Patent No. 5,955,395 (1999).
[119] A. Fukuoka, M. Ichikawa, Top. Catal. 40 (2006) 103.
[120] A. Fukuoka, J. Kimura, T. Oshio, Y. Sakamoto, M. Ichikawa, J. Am. Chem. Soc. 129 (2007) 10120.
[121] I.H. Son, M. Shamsuzzoha, A.M. Lane, J. Catal. 210 (2002) 460.
[122] K. Takamura, Y. Hiramatsu, U.S. Patent No. 6,548,034.
[123] S.H. Lee, J. Han, K.-W. Lee, Korean J. Chem. Eng. 19 (2002) 431.
[124] S.Y. Chin, O.S. Alexeev, M.D. Amiridis, J. Catal. 243 (2006) 329.
[125] H. Igarashi, H. Uchida, M. Watanabe, Chem. Lett. (2000) 1262.
[126] M.M. Schubert, M.J. Kahlich, G. Feldmeyer, M. Huttner, S. Hackenberg, H.A. Gasteiger, R.J. Behm, Phys. Chem. Chem. Phys. 3 (2001) 1123.
[127] G. Uysal, A.N. Akın, Z.İ. Önsan, R. Yıldırıma, Catal. Lett. 111 (2006) 173.
[128] O. Korotkikh, R. Farrauto, Catal. Today 62 (2000) 249.
[129] X. Liu, O. Korotkikh, R. Farrauto, Appl. Catal. A: Gen. 226 (2002) 293.
[130] M. Watanabe, H. Uchida, K. Ohkubo, H. Igarashi, Appl. Catal. B: Environ. 46 (2003) 595.
[131] A. Sirijaruphan, J.G. Goodwin Jr., R.W. Rice, J. Catal. 224 (2004) 304.
[132] M. Kotobuki, A. Watanabe, H. Uchida, H. Yamashita, M. Watanabe, J. Catal. 236 (2005) 262.
[133] M. Kotobuki, T. Shido, M. Tada, H. Uchida, H. Yamashita, Y. Iwasawa, M. Watanabe, Catal. Lett. 103 (2005) 263.
[134] K. Tanaka, Y. Moro-oka, K. Ishigure, T. Yajima, Y. Okabe, Y. Kato, H. Hamano, S. Sekiya, H. Tanaka, Y. Matsumoto, H. Koinuma, H. He, C.B. Zhang, Q.C. Feng, Catal. Lett. 92 (2004) 115.
[135] M. Shou, K. Tanaka, K. Yoshioka, Y. Moro-oka, S. Nagano, Catal. Today 90 (2004) 255.
[136] M. Shou, K.-I. Tanaka, Catal. Lett. 111 (2006) 115.
[137] A. Siani, B. Captain, O.S. Alexeev, E. Stafyla, A.B. Hungria, P.A. Midgley, J.M. Thomas, R.D. Adams, M.D. Amiridis, Langmuir 22 (2006) 5160.
[138] M. Kotobuki, A. Watanabe, H. Uchida, H. Yamashita, M. Watanabe, Appl. Catal. A: Gen. 307 (2006) 275.
[139] X. Shi, K.-I. Tanaka, H. He, M. Shou, W. Xu, X. Zhang, Catal. Lett. 120 (2008) 210.
[140] I.H. Son, A.M. Lane, Catal. Lett. 76 (2001) 151.

[141] I.H. Son, J. Power Sources 159 (2006) 1266.
[142] E. Şimşek, Ş Özkara, A.E. Aksoylu, Z.I. Ö nsan, Appl. Catal. A: Gen. 316 (2007) 169.
[143] J.L. Ayastuy, M.P. González-Marcos, J.R. González-Velasco, M.A. Gutiérrez-Ortiz, Appl. Catal. B: Environ. 70 (2007) 532.
[144] D.J. Suh, C. Kwak, J.-H. Kim, S.M. Kwon, T.-J. Park, J. Power Sources 142 (2005) 70.
[145] J. Choi, C.B. Shin, D.J. Suh, Catal. Commun. 9 (2008) 880.
[146] E.-Y. Ko, E.D. Park, K.W. Seo, H.C. Lee, D. Lee, S. Kim, Korean J. Chem. Eng. 23 (2006) 182.
[147] E.-Y. Ko, E.D. Park, K.W. Seo, H.C. Lee, D. Lee, S. Kim, J. Nanosci. Nanotechnol. 6 (2006) 3567.
[148] C. Kwak, T.-J. Park, D.J. Suh, Chem. Eng. Sci. 60 (2005) 1211.
[149] E.-Y. Ko, E.D. Park, H.C. Lee, D. Lee, S. Kim, Angew. Chem. Int. Ed. 46 (2007) 734.
[150] T. İnce, G. Uysal, A.N. Akın, R. Yıldırım, Appl. Catal. A: Gen. 292 (2005) 171.
[151] G. Uysal, A.N. Akın, Z.İ. Ö nsan, R. Yıldırım, Catal. Lett. 108 (2006) 193.
[152] W.S. Epling, P.K. Cheekatamarla, A.M. Lane, Chem. Eng. J. 93 (2003) 61.
[153] E.-Y. Ko, E.D. Park, K.W. Seo, H.C. Lee, D. Lee, S. Kim, Catal. Lett. 110 (2006) 275.
[154] S. Guerrero, J.T. Miller, E.E. Wolf, Appl. Catal. A: Gen. 328 (2007) 27.
[155] S.-H. Cho, J.-S. Park, S.-H. Choi, S.-H. Kim, J. Power Sources 156 (2006) 260.
[156] C. Kwak, T.-J. Park, D.J. Suh, Appl. Catal. A: Gen. 278 (2005) 181.
[157] Y. Minemura, S. Ito, T. Miyao, S. Naito, K. Tomishige, K. Kunimori, Chem. Commun. (2005) 1429.
[158] C. Pedrero, T. Waku, E. Iglesia, J. Catal. 233 (2005) 242.
[159] Y. Minemura, M. Kuriyama, S.-I. Ito, K. Tomishige, K. Kunimori, Catal. Commun. 7 (2006) 623.
[160] M. Kuriyama, H. Tanaka, S.-I. Ito, T. Kubota, T. Miyao, S. Naito, K. Tomishige, K. Kunimori, J. Catal. 252 (2007) 39.
[161] H.-S. Roh, H.S. Potdar, K.-W. Jun, S.Y. Han, J.-W. Kim, Catal. Lett. 93 (2004) 203.
[162] J.L. Ayastuy, M.P. González-Marcos, A. Gil-Rodríguez, J.R. González-Velasco, M.A. Gutiérrez-Ortiz, Catal. Today 116 (2006) 391.
[163] J.L. Ayastuy, A. Gil-Rodríguez, M.P. González-Marcos, M.A. Gutiérrez-Ortiz, Int. J. Hydrogen Energ. 31 (2006) 2231.
[164] O. Pozdnyakova, D. Teschner, A. Wootsch, J. Kröhnert, B. Steinhauer, H. Sauer, L. Toth, F.C. Jentoft, A. Knop-Gericke, Z. Paál, R. Schlögl, J. Catal. 237 (2006) 1.
[165] D. Teschner, A. Wootsch, O. Pozdnyakova-Tellinger, J. Kröhnert, E.M. Vass, M. Hävecker, S. Zafeiratos, P. Schnörch, P.C. Jentoft, A. Knop-Gericke, R. Schlögl, J. Catal. 249 (2007) 318.
[166] O. Pozdnyakova-Tellinger, D. Teschner, J. Kröhnert, F.C. Jentoft, A. Knop-Gericke, R. Schlögl, A. Wootsch, J. Phys. Chem. C 111 (2007) 5426.
[167] D. Teschnera, A. Wootsch, O. Pozdnyakova, H. Sauer, A. Knop-Gericke, R. Schlögl, React. Kinet. Catal. Lett. 87 (2006) 235.
[168] A. Parinyaswana, S. Pongstabodeea, A. Luengnaruemitchai, Int. J. Hydrogen Energ. 31 (2006) 1942.
[169] L. Guczi, Catal. Today 101 (2005) 53.
[170] T. Itoh, K. Kurabayashi, T. Naka, M. Takayama, O. Usaka, S. Isobe, U.S. Patent No. 6,576,208 (2003).
[171] S.Y. Chin, O.S. Alexeev, M.D. Amiridis, Appl. Catal. A: Gen. 286 (2005) 157.
[172] M. Echigo, T. Tabata, Appl. Catal. A: Gen. 251 (2003) 157.
[173] M. Echigo, T. Tabata, Catal. Lett. 98 (2004) 37.
[174] M. Echigo, T. Tabata, Catal. Today 90 (2004) 269.
[175] M. Echigo, N. Shinke, S. Takami, T. Tabata, J. Power Sources 132 (2004) 29.
[176] M. Echigo, N. Shinke, S. Takami, S. Higashiguchi, K. Hirai, T. Tabata, Catal. Today 84 (2003) 209.
[177] M. Echigo, T. Tabata, J. Chem. Eng. Jpn. 37 (2004) 558.
[178] I. Rosso, M. Antonini, C. Galletti, G. Saracco, V. Specchia, Top. Catal. 30–31 (2004) 475.
[179] G. Xu, Z.-G. Zhang, J. Power Sources 157 (2006) 64.
[180] C. Galletti, S. Fiorot, S. Specchia, G. Saracco, V. Specchia, Top. Catal. 45 (2007) 15.
[181] S.-I. Ito, T. Fujimori, K. Nagashima, K. YuzaKi, K. Kunimori, Catal. Today 57 (2000) 247.
[182] S.-I. Ito, H. Tanaka, Y. Minemura, S. Kameoka, K. Tomishige, K. Kunimori, Appl. Catal. A: Gen. 273 (2004) 295.
[183] W. Zhang, A. Wang, L. Li, X. Wang, T. Zhang, Catal. Lett. 121 (2008) 319.
[184] Y. Huanga, A. Wang, X. Wang, T. Zhang, Int. J. Hydrogen Energ. 32 (2007) 3880.
[185] J.S. Wainright, M.H. Litt, R.F. Savinell, in: W. Vielstich, A. Lamm, H.A. Gasteiger (Eds.), Handbook of Fuel Cells: Fundamentals Technology and Applications, vol. 3, John Wiley & Sons Ltd., West Sussex, 2003, , p. 436part 2.
[186] J.L. Zhang, Z. Xie, J.J. Zhang, Y.H. Tanga, C.J. Song, T. Navessin, Z.Q. Shi, D.T. Song, H.J. Wang, D.P. Wilkinson, Z.S. Liu, S. Holdcroft, J. Power Sources 160 (2006) 872.
[187] P. Jannasch, Curr. Opin. Colloid Interf. Sci. 8 (2003) 96.
[188] Q. Li, R. He, J.O. Jensen, N.J. Bjerrum, Chem. Mater. 15 (2003) 4896.
[189] K. Rutt, M. Vogt, R. Zuber, in: W. Vielstich, A. Lamm, H.A. Gasteiger (Eds.), Handbook of Fuel Cells: Fundamentals Technology and Applications, vol. 3, John Wiley & Sons Ltd., West Sussex, 2003, , p. 489part 2.